BNL 27899
CONF-800243--1

AN EFFECTIVE MASS TRIGGER AT THE BROOKHAVEN MULTI-PARTICLE SPECTROMETER (MPS)*

Contribution to the Wire Chamber Conference, Vienna

February 27 - 29, 1980

Erich H. Willen

Brookhaven National Laboratory
Upton, New York 11973

* This work was performed under contract number DE-AC02-76CH00016 with the U.S. Department of Energy.

Introduction

Experiments at the Brookhaven MPS[1] are able to generate large amounts of data which must be processed on general purpose computers. The cost of this processing is high and can set an effective limit on the sensitivity of a particular experiment, forcing an experimenter to make compromises in the design of his experiment which he would not otherwise make. This problem will become particularly severe with the introduction of the MPS II drift chamber detector system,[2] where the allowed beam rates will be $\sim$ 10 times higher than those previously used in the MPS. The effective mass trigger (EMT),[3] currently under development at Brookhaven, is a device designed to help alleviate this problem. The goal is to decide on the presence of a desired effective mass in a particle reaction in < 500 μs, with high efficiency.

In the EMT, the pattern of hits in several proportional wire chambers (PWC) is used to give addresses for table lookup of momentum components. A microprocessor then reconstructs the effective mass from these momentum components. During this period, the electronic system is digitizing the track information for all the MPS detectors, and storing it in memory. At any time, the event encoding can be aborted and the digitizers reset to accept the next event. Alternately, the event can be written on tape with a flag indicating the results of the EMT calculation and this information used in later data analysis.

This trigger would be generally useful in most MPS experiments since virtually all of them search for an effective mass at some stage in the analysis. The EMT concept need not be restricted to a search for effective mass, however; it could equally well be used to look for other kinematic quantities of interest in a particular experiment.

The goal here is different than the one usually sought in software/pattern recognition/special processor systems. It is not necessary to achieve high resolution or 100% efficiency, but rather, sufficient selectivity to choose events with good probability of containing kinematics unique to the reaction being studied. In this spirit, approximations are permitted which are not normally appropriate in analysis systems. The purpose of this paper is to show how an EMT trigger would work at the MPS and to show what its resolution would be.

Multi-Particle Spectrometer (MPS)

A layout of the MPS is shown in Fig. 1. Included is a large aperture dipole magnet with a 10kG field over a volume 122 x 183 x 457 cm^3. The field has variations of $\sim$ 25% in the magnet midplane.[4] The field volume is normally filled with detectors which can easily be configured for the needs of a particular experiment. With the MPS II drift chamber system, useful beam rates of $\sim 2 \times 10^6$/pulse will become feasible.

Triggers at the MPS are made up of multiplicity-counting PWC's and scintillation counters, Cerenkov counters, and in one experiment, a transition radiator and shower counter. A recent addition to this list has been the RAM,[5] a random-access memory which is able to select momenta by comparing the hits in a set of three detectors with patterns stored in memory. These devices have generally produced trigger rates on the order of 1/10K to 1/50K, with 1/100K being achieved only rarely, and for very special topologies. In MPS II, we thus would have data rates of 40-200 events/2.4 sec., leading to 30×10^6 - 150×10^6 events in a 500 hour experiment. At 0.5 sec/event processing time on a CDC 7600 computer, this data rate becomes unfeasible.

Effective Mass Trigger (EMT)

Fig. 2 is a drawing of the basic detector elements of the EMT. A target is centered at z = 0, inside the MPS field volume.

D_a, D_{bx} and D_c have vertical wires spaced .254 cm and measure the X coordinate. D_{by} has horizontal wires spaced .254 cm and measures the Y coordinate. D_{bu} has wires 10° to the vertical. Wire hits in the two detectors D_a and D_{bx} together with the point z = 0, define a unique P_x, P_z. The wire hits are used as an address to look up in a memory, the value of P_x and P_z. Stored at the same address is also the sign of the track for that combination of hits and the appropriate range of hits in D_c, allowing most false combinations to be rejected. D_{bx} and D_{by} are used as an address to find, in a second memory, the appropriate hit in D_{bu}, thus correlating x with y in D_b. P_z and D_{by} are used as the address for getting P_y from a third memory. These memory words are shown in Fig. 3.

For each event, two lists are assembled: one for positive tracks and one for negative tracks. The microprocessor then combines these tracks into effective masses and allows the recording of the event to proceed if it finds an effective mass in the appropriate range. Preliminary estimates indicate this decision can be made in a suitably short time using a device such as the Motorola 68000 microprocessor.

The use of a point target in this concept leads to considerable simplification over other possible schemes for getting momentum components quickly. Since experiments use targets of finite length (usually 60 cm in the MPS), errors are introduced which can become significant. However, enough precision is retained that this approach proves useful. Another source of error is the x, y position of the interaction in the target. However,

a displacement from the point $x = y = 0$, used in generating the tables, can be compensated using information from the incident beam chambers.

Momentum Resolution

Figures 4 and 5 give the momentum error for the detector layout of Fig. 2. In Figs. 4 and 5, the ordinate is a difference: the momentum of a track as found by table lookup subtracted from the correct momentum for that track. Figure 4 gives ΔP_z for tracks originating at $z = 10$ cm when $z = 0$ is used in generating the tables. Tracks with large $|z|$ and large $|P_x|$ have the largest error, as might be expected. Not shown is the error associated with the finite detector resolution which is, in most cases, small compared to the error caused by the displacement of the z origin of the track. There is little dependence of the error ΔP_x on P_z, only on z (Fig. 5).

Figures 4 and 5 are for positive tracks. Such tracks originating with negative P_x tend to have the smallest ΔP_x (the opposite is the case for negative particles). This improves the accuracy with which a two-body effective mass can be reconstructed, and it is precisely this topology (topology A, Fig. 2) which has favorable acceptance in the MPS.

The curves of Figs. 4 and 5 are illustrative of the tendency of the errors but are generally not useful for specific calculations because there are sizable errors on the curves and they are calculated for specific tracks (e.g. $P_y = 0$ for Fig. 4 and Fig. 5).

Effective Mass and Mass Resolution

The invariant mass squared of two particles i and j is

$$S_{ij} \equiv M_{ij}^2 = (E_i + E_j)^2 - (\vec{P}_i + \vec{P}_j)^2, \tag{1}$$

where E is the energy and $\vec{P}$ is the vector momentum. Expanding (1),

$$S_{ij} = (E_i + E_j)^2 - (P_{ix} + P_{jx})^2 - (P_{iy} + P_{jy})^2 - (P_{iz} + P_{jz})^2 \tag{2}$$

E_i is given by

$$E_i^2 = P_{ix}^2 + P_{iy}^2 + P_{iz}^2 + M_i^2,$$

and likewise for E_j. To solve (2), given the momentum components, requires 13 add or subtract, 10 squaring, and 2 square root operations.

Equation (1) can be rewritten to give

$$S_{ij} = M_i^2 + M_j^2 + 2\,(E_iE_j - P_{ix}P_{jx} - P_{iy}P_{jy} - P_{iz}P_{jz}) . \tag{3}$$

Differentiating (3) and neglecting the cross terms:

$$\delta S_{ij} \approx a_1 a_2 + b_1 b_2 + c_1 c_2 + d_1 d_2 + e_1 e_2 + f_1 f_2 \tag{4}$$

where

$$a_1 = 2\,(R_{ji}P_{ix} - P_{jx}) \quad ; \quad a_2 = \delta P_{ix}$$

$$b_1 = 2\,(R_{ij}P_{jx} - P_{ix}) \quad ; \quad b_2 = \delta P_{jx}$$

$$c_1 = 2\,(R_{ji}P_{iy} - P_{jy}) \quad ; \quad c_2 = \delta P_{iy}$$

$$d_1 = 2\,(R_{ij}P_{jy} - P_{iy}) \quad ; \quad d_2 = \delta P_{jy}$$

$$e_1 = 2\,(R_{ji}P_{iz} - P_{jz}) \quad ; \quad e_2 = \delta P_{iz}$$

$$f_1 = 2\,(R_{ij}P_{jz} - P_{iz}) \quad ; \quad f_2 = \delta P_{jz}$$

and $R_{ji} = P_j/P_i$

$R_{ij} = P_i/P_j$.

Since

$$\delta S_{ij} = \delta (M_{ij})^2,$$

$$\delta M_{ij} \approx \frac{\delta S_{ij}}{2M_{ij}} . \qquad (5)$$

In practice, all the terms in (4) can contribute significantly to the error δS_{ij}. The e and f terms, however, tend to cancel. Also, while the δP_z can be large, their coefficients are small. The a and b terms usually contribute most because of the coefficients of the δP_x. These terms, furthermore, contribute with like sign. These errors are systematic errors, caused by the target length.

Specific Example

An example of a reaction which has been studied in some detail is the following:

$$18\text{Gev/c} \quad \pi^- p \to \bar{D}^{*-} C^+ \qquad (R1)$$
$$\hookrightarrow \bar{D}^0 \pi^-$$
$$\hookrightarrow K^+ \pi^-$$

with $M(D^0) = 1.86$ Gev.

The performance of the EMT for this $\bar{D}^0$ will be shown, derived by Monte Carlo simulation.

Figure 6 shows the resolution this trigger would achieve for topology A, using 60 cm target length (mass resolutions are S.D.). The solid histogram assumes the x, y position in the target has been corrected to ±0.5 mm using beam information. The dashed histogram assumes no x,y correction has been made and thus, the events originate in x,y according to the beam profile. The resolution is still acceptable; few events of this topology are lost for a mass cut of ± 10% in the trigger.

Figure 7 shows how the resolution varies with position in the target. Over 2/3 of the accepted events have topology A, and for these the resolution is best. For topology B, the resolution is worse, and some loss of events originating in the ends of the target will occur.

Figures 6 and 7 are for events accepted in the MPS detector system (exclusive of the EMT) for reaction (R_1), and this forms a limited subset of all possible $\bar{D}_o$ decays.

Table I lists the relevant parameters for 5 $\bar{D}^o$ decays accepted in the apparatus. Included are the quantities (momentum modulus 25 MeV/c) from table lookup as would be used in the EMT calculation.

The effective mass resolution formulas (4) and (5) can be applied to this reaction. Table 2 gives the error terms for the 5 events of Table I. There is good agreement with the Monte Carlo derived errors shown in Fig. 7.

Conclusion

Figure 6 shows that the resolution which can be achieved is quite adequate to make the EMT useful in this reaction. Other effective masses have been studied and similar encouraging results found. The $\bar{D}^o$ of reaction (R_1), with its large Q value, produces tracks with sizable P_x and thus is a stringent test of the efficacy of this trigger. The mass resolution for a reaction such as $\phi \rightarrow 2K$ will be considerably better. Because of the multi-dimensional nature of this problem, it is in general necessary to carry out extensive calculations to properly assess the performance of this trigger in a particular reaction; studying an isolated event or two can easily lead to the wrong conclusions, pro or con.

For the reaction (R_1), a careful study of existing MPS data shows that a reduction of greater than 10 in its rate can be achieved over the best

alternate trigger. Even larger reductions have been found for other reactions. Thus, the EMT is a potentially powerful tool in the struggle against unwanted data and ever rising computer processing costs.

The extensive experience of the members of the Lindenbaum/Ozaki Group with the MPS and its requirements has provided the impetus for the development of this concept.

References

1. E.D. Platner et al., Proc. of the Int. Conf. on Instrumentation for High Energy Physics, Frascati, Italy, May 8-11, 1973, Ed. S. Stipcich (Laboratori Nazionali del Comitato Nazionale per l'Energia Nucleare, Servizio Documentazione, Frascati, Italy, 1973), p. 672; S. Ozaki, BNL Report #25311 and Recent Bubble Chamber Physics (Proc. of the Int. Symp. held at Tohoku University, Sendai, Japan, August 17-18, 1978) Eds. S. Tanaka and K. Tamai, pgs. 179-205.

2. E.D. Platner, IEEE Transactions on Nuclear Science, Vol. NS-25, pgs. 35-37, February 1978; A. Etkin, IEEE Transactions on Nuclear Science, Vol. NS-26, pgs. 54-58, February 1979.

3. E. Willen, An Effective Mass Trigger at the MPS, September 11, 1979, MPS Report #52.

4. W.A. Love, An Atlas of MPS Field Plots, June 6, 1979, MPS Report #50.

5. E.D. Platner, IEEE Transactions on Nuclear Science, Vol. NS-24, pg. 225, February 1977.

Tables

Table 1: A table of typical events for the decay $\bar{D}^{o}(1865) \rightarrow K^{+} \pi^{-}$, produced at various z in the MPS. Under P_{gen} are listed the momentum components for the positive and negative tracks as well as the wire number they strike in D_a and D_{bx}. Under P_{rec} are listed the momentum components obtained by table lookup. The last two columns are the mass calculated from these components, in units of 25 Mev, and this mass converted to Gev.

Table 2: A list of the errors in the momentum components due to the difference between the true momentum and that stored for the relevant combination of hits in D_a, D_{bx}, D_{by}, for the events of Table 1. The 6 error terms a to f of (4), and the term δM_{ij} of (5) are also given.

Table 1

z(cm)	Ev#	P_{gen}, GeV/c i = +					P_{gen}, GeV/c j = -					P_{rec}, (25 Mev/c) i = +			P_{rec}, (25 Mev/c) j = -				
		P_x	P_y	P_z	D_a	D_{bx}	P_x	P_y	P_z	D_a	D_{bx}	P_x	P_y	P_z	P_x	P_y	P_z	M	Mx.025
-30	1	-1.06	.26	8.95	121	269	.61	-.35	5.25	246	351	-39	9	284	23	-12	182	70	1.74
-10	2	-1.17	.11	7.12	96	224	.54	-.18	6.84	225	339	-45	4	260	21	- 7	260	73	1.83
0	3	.61	-.40	6.75	301	635	-.53	.88	6.79	100	89	23	-16	262	-20	34	264	72	1.81
10	4	- .42	.21	7.90	183	384	.97	-.63	5.92	283	455	-17	9	335	40	-25	253	76	1.90
30	5	- .88	-.47	6.47	132	280	.35	.67	7.77	205	316	-39	-22	339	16	27	350	80	1.99

Table 2

z(cm)	Ev#	i = +			j = -									
		δP_x	δP_y	δP_z	δP_x	δP_y	δP_z	a	b	c	d	e	f	δM_{ij}
-30	1	-.094	.042	1.85	.033	-.037	.708	.116	.070	.021	.032	.014	-.009	.131
-10	2	-.046	.004	.618	.010	-.004	.327	.076	.017	.001	.001	-.042	.023	.041
0	3	.031	.002	.204	-.022	.030	.188	.036	.025	-.002	.038	.008	-.007	.053
10	4	.019	-.007	- .473	-.021	.002	- .410	-.025	-.036	-.006	-.002	-.048	.054	-.034
30	5	.101	.090	-2.00	-.045	-.012	- .973	-.141	-.053	-.111	-.013	.109	-.044	-.136

FIGURE CAPTIONS

Fig. 1 Layout of the MPS, showing the magnet and some of the downstream detectors normally used in experiments.

Fig. 2 Layout of the detectors used for the effective mass trigger calculations. The detectors D are proportional wire chambers with wire spacing 0.254 cm. D_a and D_c measure the x-coordinate. An event with topology A has a generally higher acceptance in the MPS.

Fig. 3 A possible organization of the memories containing the momentum information needed for the EMT. The numbers are the estimated number of bits required.

Fig. 4 Error in P_z for tracks originating at z = 10 cm with table origin z = 0. ΔP_z is the difference obtained by subtracting the momentum stored in the table from the correct track momentum. The error is a strong function of P_x, which is marked on the curves. The plots are for positive tracks with $P_y = 0$. For negative tracks, reverse the sign of P_x.

Fig. 5 Error in P_x for positive tracks with $P_y = 0$ originating at various z positions relative to the table origin z = 0. The error is nearly independent of P_z. For negative tracks, reverse the sign of P_x and ΔP_x.

Fig. 6 Mass reconstructed by EMT (M) subtracted from true mass M_o vs. z position relative to table origin, for the decay $\bar{D}^o(1865) \rightarrow K^+\pi^-$ in the MPS. Events with topology A have good acceptance in the MPS; events with topology B have poorer acceptance, particularly for negative z.

FIGURE CAPTIONS (continued)

Fig. 7 Trigger resolution in effective mass for $\bar{D}^0 \to K^+\pi^-$, topology A, 60 cm long target. Solid histogram has events originating with the target x, y = ± .5 mm. Dashed histogram has x, y target position spread according to beam profile.

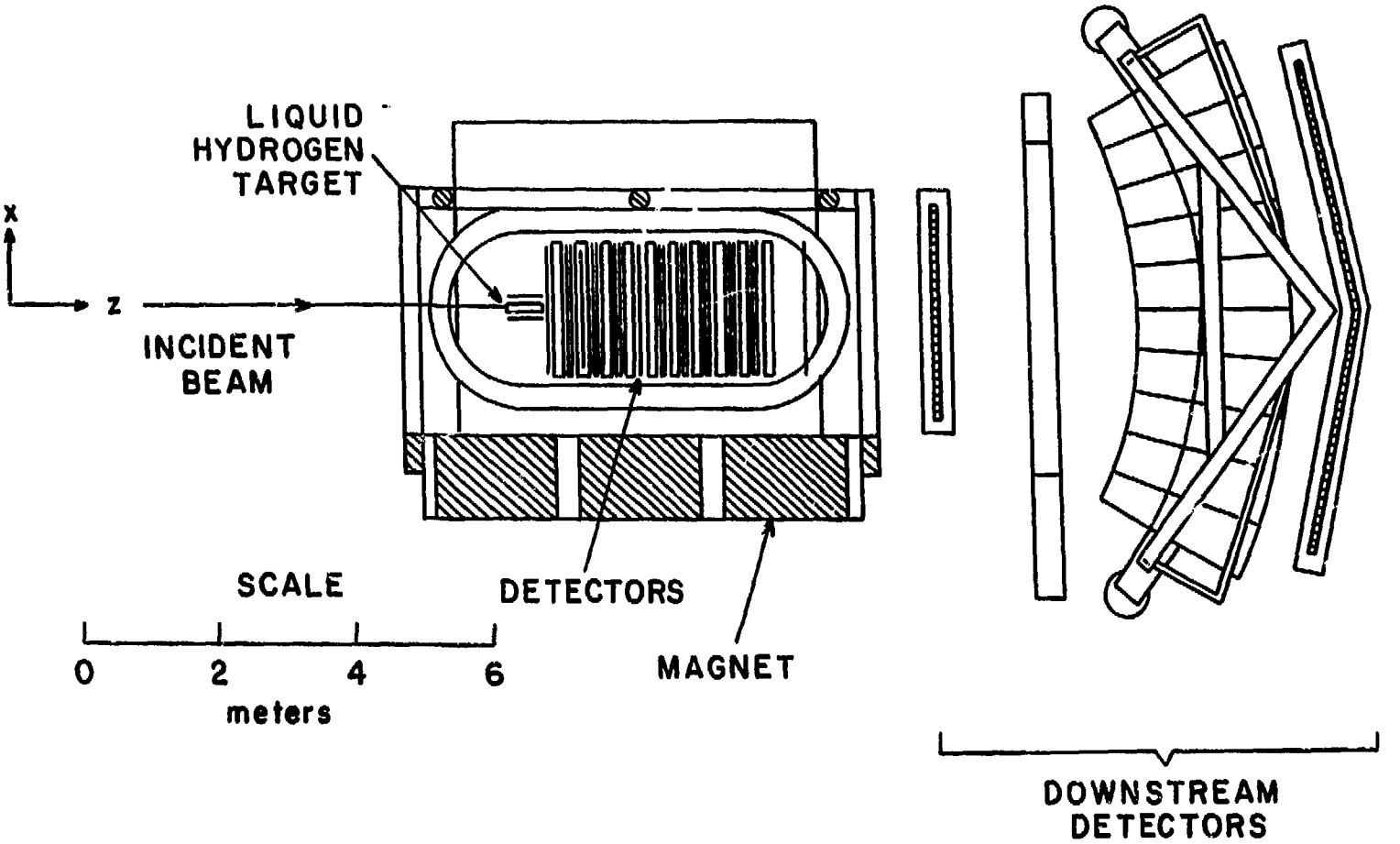
LIQUID
HYDROGEN
TARGET
X
Z
INCIDENT
BEAM
SCALE
0
2
4
6
meters
DETECTORS
MAGNET
DOWNSTREAM
DETECTORS

Figure 1

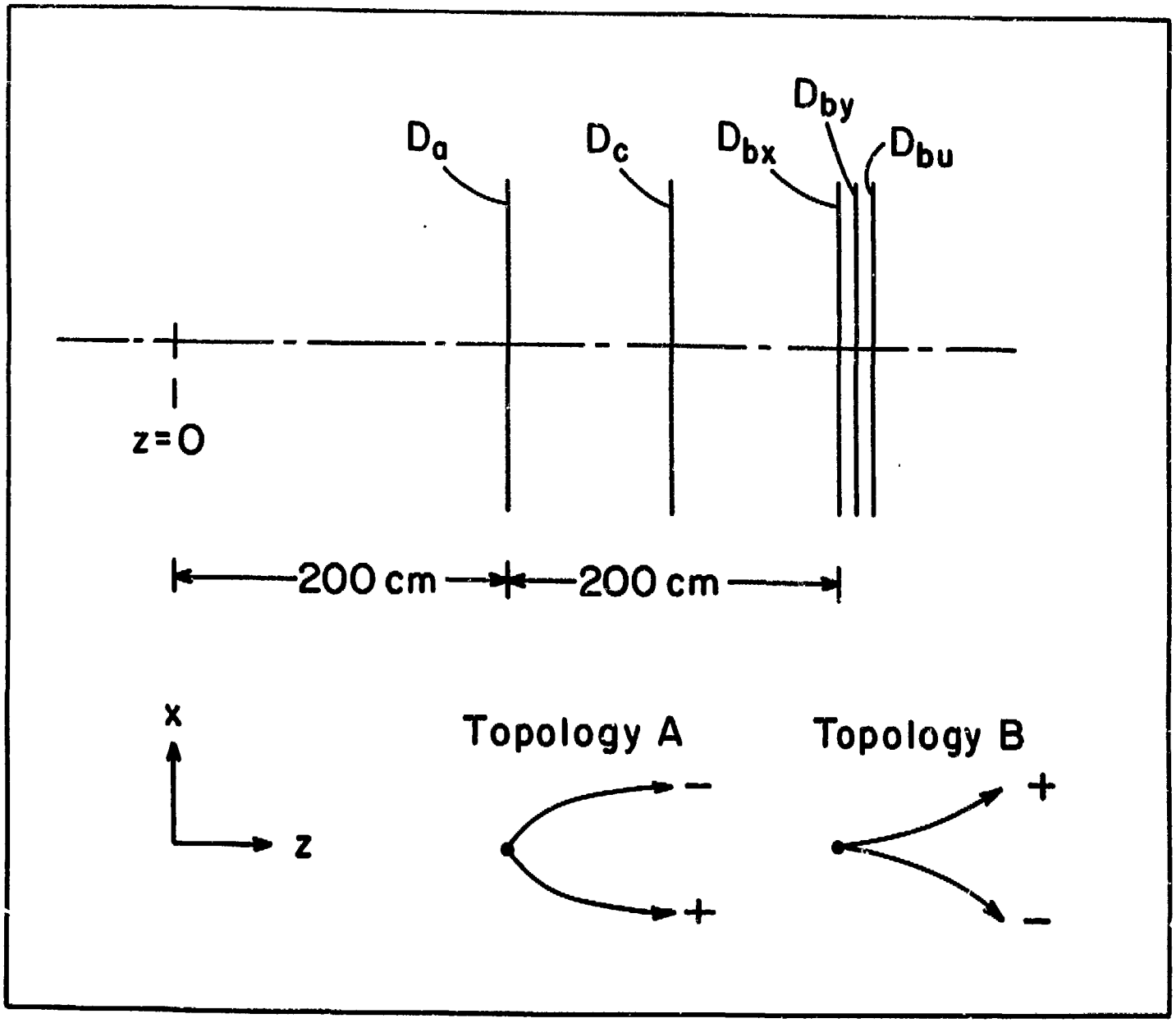

Figure 2

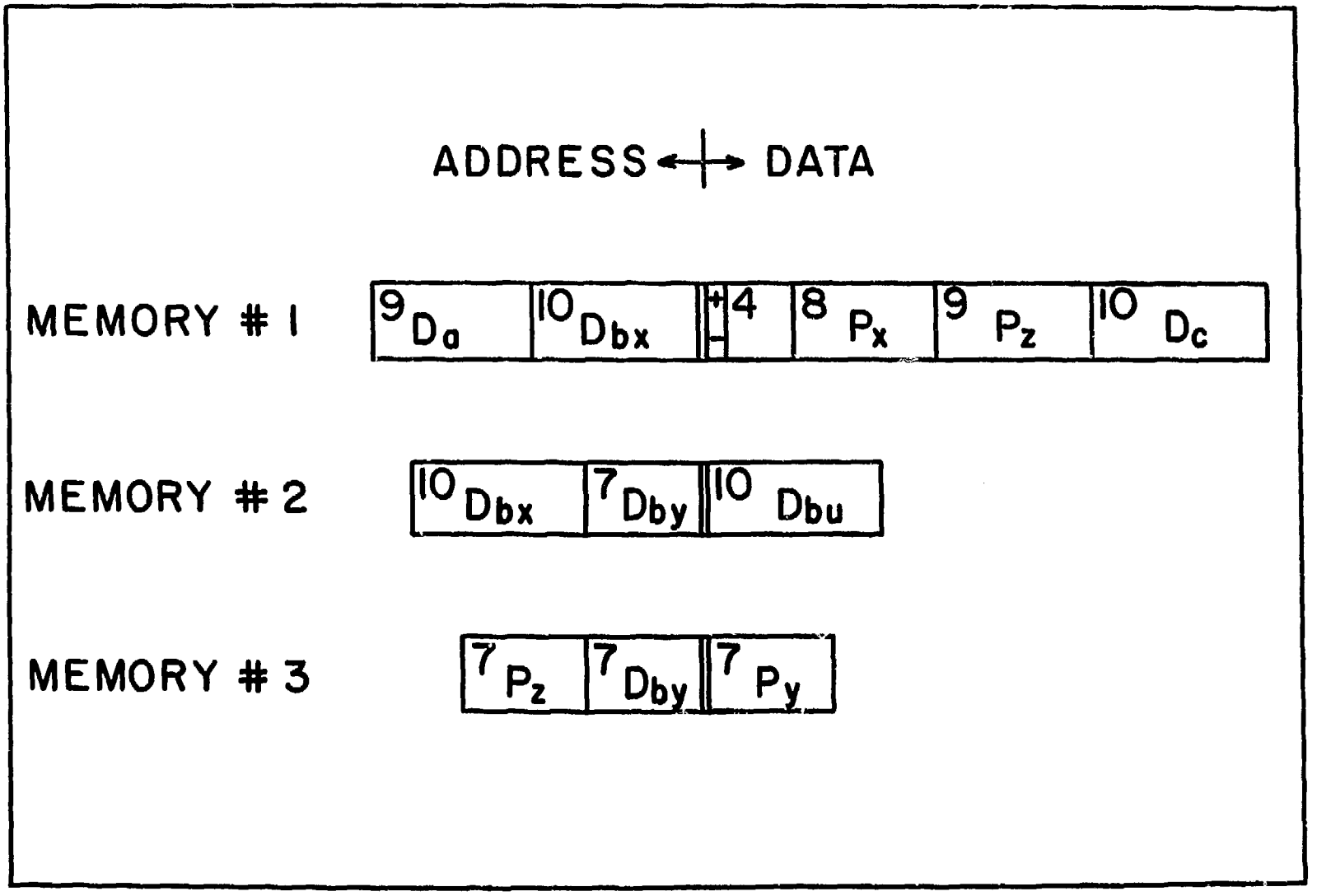
ADDRESS
DATA
MEMORY # 1
9 Da
10 Dbx
4
8 Px
9 Pz
10 Dc
MEMORY # 2
10 Dbx
7 Dby
10 Dbu
MEMORY # 3
7 Pz
7 Dby
7 Py

Figure 3

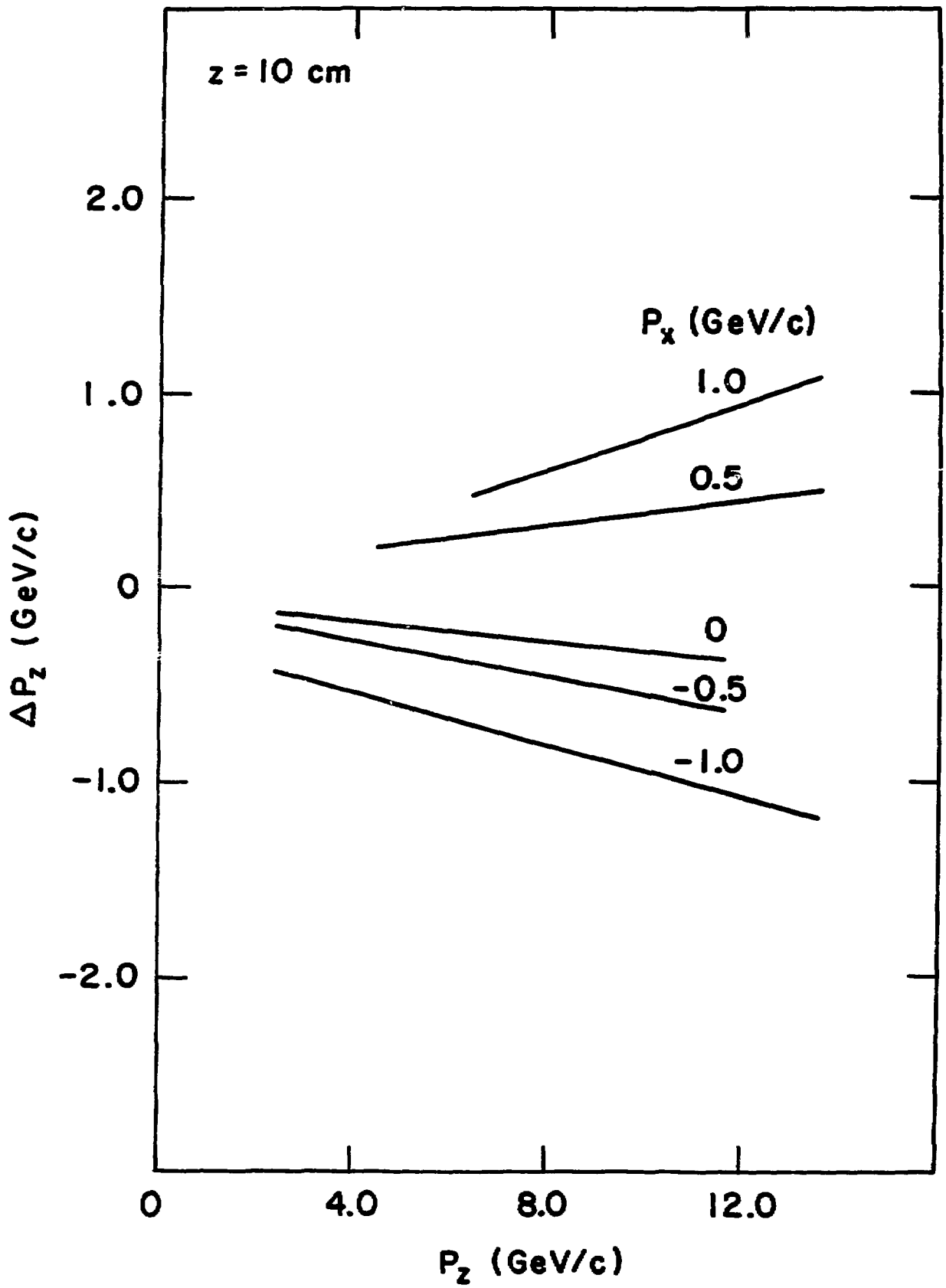
z = 10 cm
2.0
1.0
0
-1.0
-2.0
ΔPz (GeV/c)
Px (GeV/c)
1.0
0.5
0
-0.5
-1.0
0
4.0
8.0
12.0
Pz (GeV/c)

Figure 4

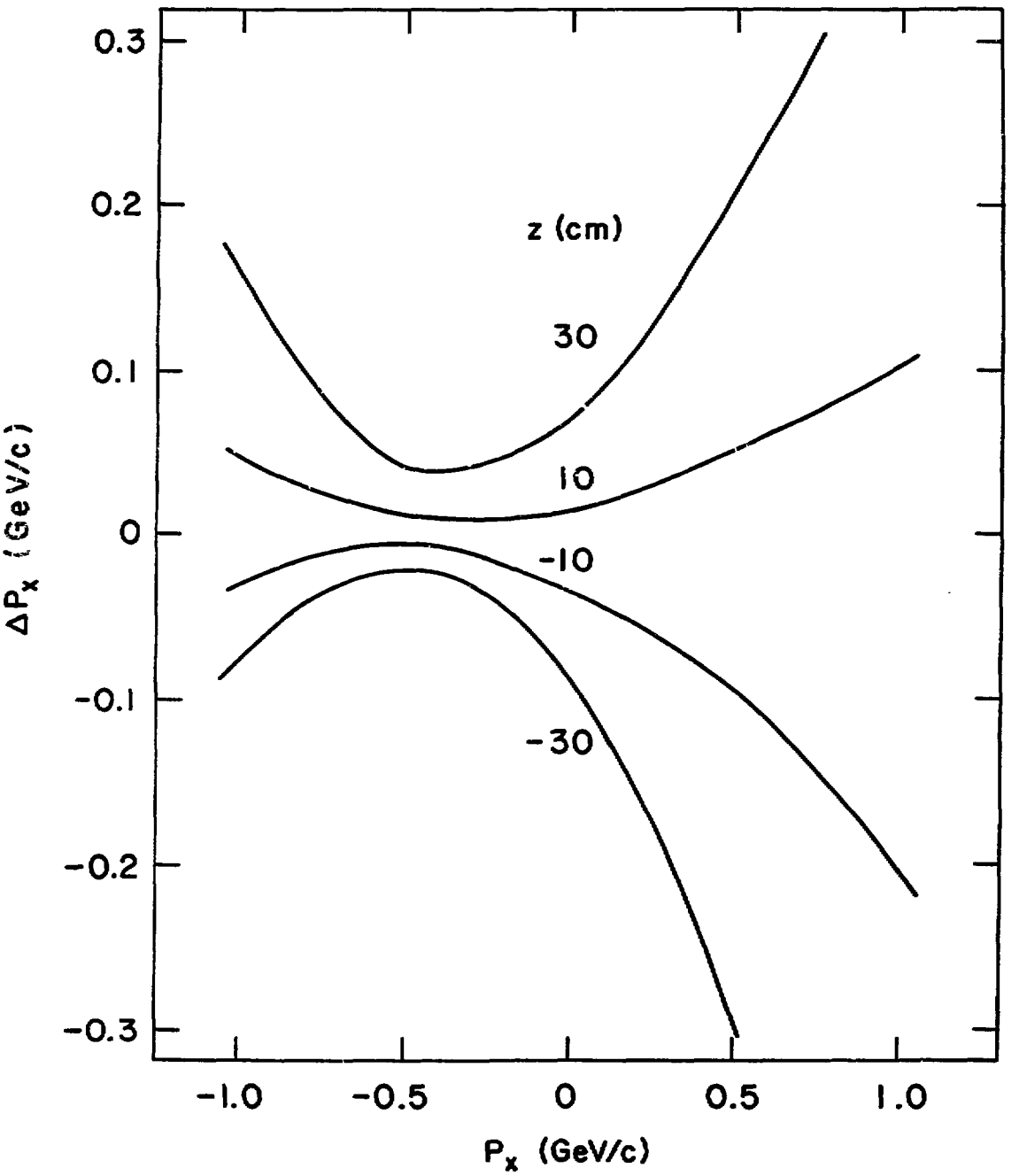

Figure 5

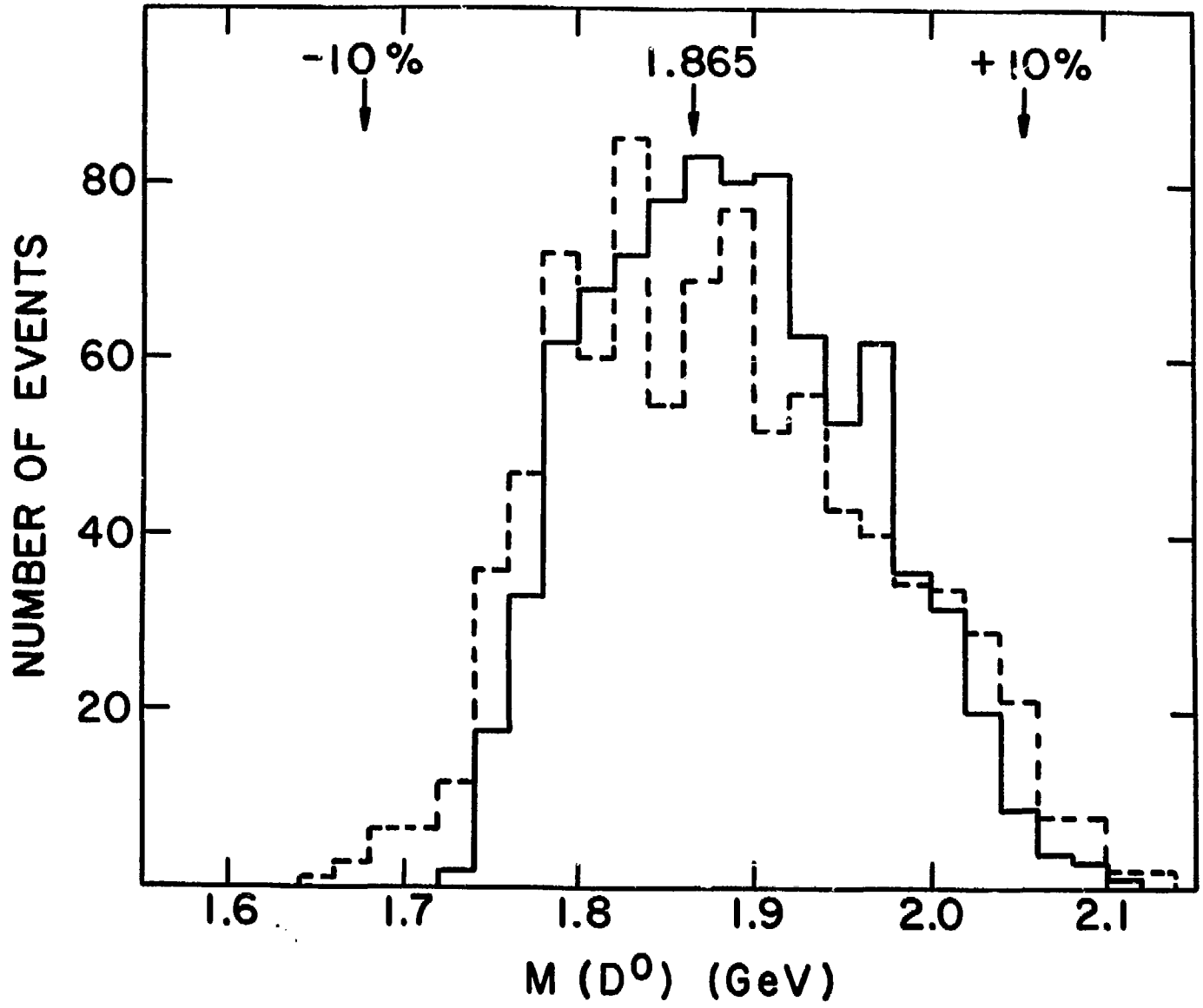

Figure 6

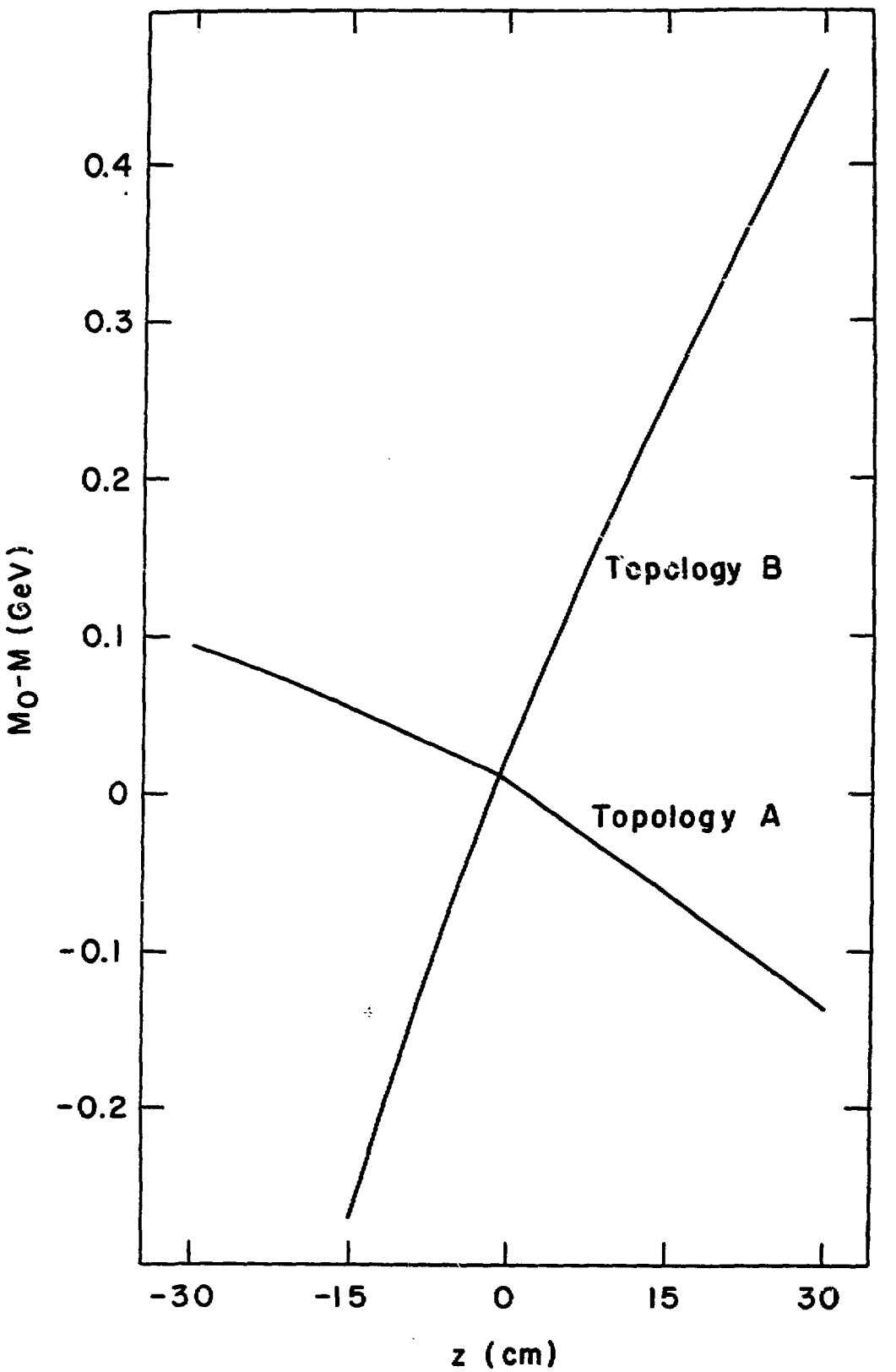

Figure 7